

LETTER

Tistarite,  $\text{Ti}_2\text{O}_3$ , a new refractory mineral from the Allende meteorite

CHI MA\* AND GEORGE R. ROSSMAN

Division of Geological and Planetary Sciences, California Institute of Technology, Pasadena, California 91125, U.S.A.

ABSTRACT

Tistarite, ideally  $\text{Ti}_2\text{O}_3$ , is a new member of the corundum-hematite group. It is found as one subhedral crystal in a cluster of micrometer-sized refractory grains along with khamrabaevite (TiC), rutile, and corundum crystals within a chondrule from the Allende meteorite. The mean chemical composition determined by electron microprobe analysis is (wt%)  $\text{Ti}_2\text{O}_3$  94.94, MgO 2.06,  $\text{Al}_2\text{O}_3$  1.50,  $\text{ZrO}_2$  0.44, FeO 0.24, CaO 0.10,  $\text{Cr}_2\text{O}_3$  0.06, sum 99.34. The empirical formula calculated on the basis of 3 O atoms is  $(\text{Ti}_{1.90}^{3+}\text{Mg}_{0.07}\text{Al}_{0.04}\text{Zr}_{0.01})_{\Sigma 2.02}\text{O}_3$ . Tistarite is rhombohedral,  $R\bar{3}c$ ;  $a = 5.158 \text{ \AA}$ ,  $c = 13.611 \text{ \AA}$ ,  $V = 313.61 \text{ \AA}^3$ , and  $Z = 6$ . Its electron back-scatter diffraction pattern matches that of synthetic  $\text{Ti}_2\text{O}_3$  with the  $R\bar{3}c$  structure. The strongest calculated X-ray powder diffraction lines from the synthetic  $\text{Ti}_2\text{O}_3$  data are [ $d$  spacing in  $\text{Å}$  ( $hkl$ ): 3.734 (84) (012), 2.707 (88) (104), 2.579 (90) (110), 2.242 (38) (113), 1.867 (33) (024), 1.703 (100) (116), 1.512 (28) (214), 1.489 (46) (300), 1.121 (20) (226), 0.896 (25) (416)]. The mineral is named after the composition “Ti” and the word “star,” implying that this new refractory mineral is among the first solids formed in the solar system.

**Keywords:** Tistarite,  $\text{Ti}_2\text{O}_3$ , new refractory mineral, titanium oxide, Allende meteorite

INTRODUCTION

During a nanomineralogy investigation of the Allende meteorite, a new titanium oxide mineral,  $\text{Ti}_2\text{O}_3$ , was discovered in a corundum-rich cluster of refractory grains in situ in an Allende chondrule. Electron microprobe, high-resolution SEM, electron back-scatter diffraction (EBSD), EDS, and Raman analyses have been used to characterize its composition and structure. Synthetic  $\text{Ti}_2\text{O}_3$  is well known in the field of materials science. We report the first occurrence of  $\text{Ti}_2\text{O}_3$  in nature.

MINERAL NAME AND TYPE MATERIAL

The mineral and the mineral name have been approved by the Commission on New Minerals, Nomenclature and Classification (CNMNC) of the International Mineralogical Association (IMA 2008-016). The name of the new mineral is derived from the word “star” and the composition “Ti,” implying that this new mineral is likely a condensate among the first solids formed in the solar system at the birth of our star. The thin section containing the holotype material is in the collection of the Smithsonian Institution’s National Museum of Natural History and is catalogued under USNM 3510-6.

OCCURRENCE, ASSOCIATED MINERALS, AND ORIGIN

Tistarite occurs as one isolated grain within a cluster of refractory grains discovered in situ in a ferromagnesian chondrule from the Allende meteorite, along with about 30 corundum ( $\text{Al}_2\text{O}_3$ ) grains, one khamrabaevite (TiC) grain, one rutile ( $\text{TiO}_2$ ) grain, and one mullite grain ( $\text{Al}_6\text{Si}_2\text{O}_{13}$ ) (Figs. 1–2). This cluster is about 130  $\mu\text{m}$  in diameter inside a  $1.3 \times 1.4 \text{ mm}$  chondrule in the section plane. Mg-rich olivine ( $\text{Fo}_{99-93}$ ) occupies the core

area of the chondrule with a rim consisting of enstatite and more Fe-rich olivine ( $\text{Fo}_{81-61}$ ), surrounded by matrix of mainly olivine and troilite. The mineral has been found, to date, within only one chondrule in one polished Allende section. The Allende meteorite, which fell at Pueblito de Allende, Chihuahua, Mexico, on February 8, 1969, is a CV3 carbonaceous chondrite.

APPEARANCE, PHYSICAL AND OPTICAL PROPERTIES

One subhedral tistarite crystal was first recognized by its stronger back-scattered electron intensity within a chondrule in the scanning electron microscope (Figs. 1–2). Back-scatter electron (BSE) images were obtained both with a ZEISS 1550VP field-emission SEM and a JEOL 8200 electron microprobe using solid-state BSE detectors. Tistarite occurs as an  $\sim 5 \times 7 \mu\text{m}$  grain, which is the type specimen. It is gray in reflected light and opaque in transmitted light. Streak, luster, hardness, tenacity, cleavage, fracture, and density were not determined due to the small grain size. It is non-fluorescent under the beams of the electron microprobe and SEM. The calculated density is  $4.53 \text{ g/cm}^3$ , using the empirical formula. Neither crystal forms nor twinning was observed. The  $a:c$  ratio calculated from the unit-cell parameters is: 1:2.6388.

Nano-inclusions have been observed in this tistarite grain by high-resolution BSE imaging (Fig. 3). Their EBSD patterns could not be obtained. Based on the bulk composition of this grain, the platy uniformly distributed inclusions are probably  $\text{MgTi}_3^+\text{O}_4$ , a new spinel-group mineral. To protect the only type-material grain, TEM is not used to investigate the nano-inclusions through a destructive focused ion beam sample preparation.

CHEMICAL COMPOSITION

Chemical analyses (5) were carried out by means of the JEOL 8200 electron microprobe (WDS mode, operated at 15 kV and

\* E-mail: chi@gps.caltech.edu

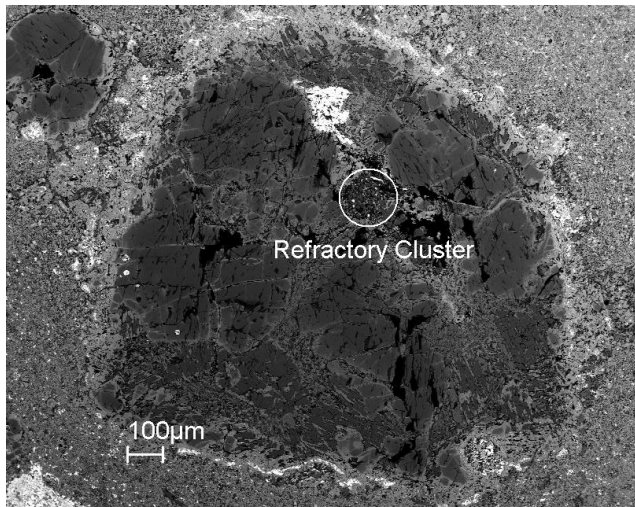


**FIGURE 1.** Back-scattered electron image of the cluster of refractory grains inside a chondrule in a polished section (USNM 3510-6) of the Allende meteorite.

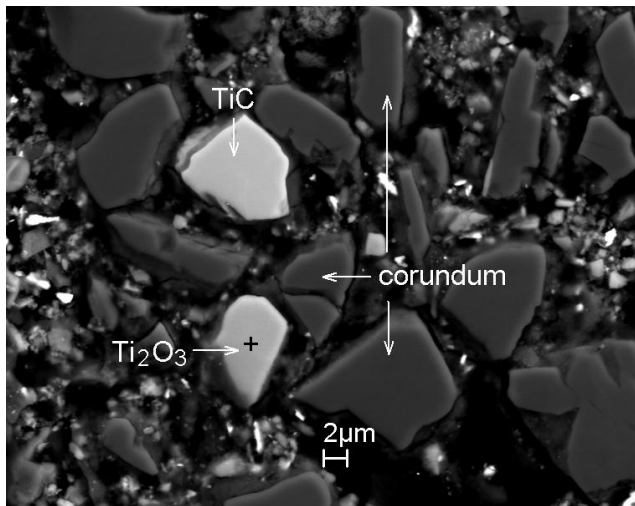


**FIGURE 2.** Enlarged back-scattered electron image showing one tistarite ( $\text{Ti}_2\text{O}_3$ ) grain along with khamrabaevite (TiC) and corundum. The cross marks where the electron back-scattered diffraction pattern (shown in Fig. 4) was collected.

10 nA in a focused beam mode). Standards for the analysis were  $\text{TiO}_2$  (TiK $\alpha$ ), forsterite (MgK $\alpha$ ), zircon (ZrL $\alpha$ ), anorthite (CaK $\alpha$ , AlK $\alpha$ ), fayalite (FeK $\alpha$ ),  $\text{Cr}_2\text{O}_3$  (CrK $\alpha$ ), and Hf metal (HfL $\alpha$ ). Analyses were processed with the CITZAF correction procedure (Armstrong 1995). No other elements with atomic number >4 were detected by WDS scans. The mean analytical results of all 5 analyses (Table 1) provide the empirical formula, which, based on 3 O atoms per formula unit, is  $(\text{Ti}_{1.90}^{3+}\text{Mg}_{0.07}\text{Al}_{0.04}\text{Zr}_{0.01})_{\Sigma 2.02}\text{O}_3$  where Ti is only 3+. The ideal end-member formula is  $\text{Ti}_2\text{O}_3$ .

#### CRYSTALLOGRAPHY BY ELECTRON BACK-SCATTER DIFFRACTION

The tistarite crystal is too small for conventional single-crystal or powder XRD study and would be difficult to extract from its accompanying grains. Single-crystal electron back-scatter diffraction (EBSD) analyses at a submicrometer scale were

**TABLE 1.** Electron microprobe analyses of tistarite

Constituent	wt%	Range	Std. dev.	Probe standard
$\text{Ti}_2\text{O}_3$	94.94	94.56–95.37	0.34	$\text{TiO}_2$
MgO	2.06	2.00–2.12	0.05	spinel
$\text{Al}_2\text{O}_3$	1.50	1.40–1.57	0.07	anorthite
$\text{ZrO}_2$	0.44	0.37–0.52	0.06	zircon
FeO	0.24	0.20–0.25	0.02	hematite
CaO	0.10	0.09–0.11	0.01	anorthite
$\text{Cr}_2\text{O}_3$	0.06	0.03–0.09	0.03	$\text{Cr}_2\text{O}_3$
$\text{HfO}_2$	0.02	0.00–0.06	0.03	Hf metal
Total	99.36			

performed using a HKL EBSD system on the ZEISS 1550VP scanning electron microscope, operated at 20 kV and 8 nA in a focused beam with a 70° tilted stage. The EBSD system was calibrated using a single-crystal silicon standard. The structure was determined and cell constants were obtained by matching the experimental EBSD pattern with the structures of synthetic  $\text{Ti}_2\text{O}_3$  (Vincent et al. 1980; Rice and Robinson 1977; Newnham and de Haan 1962), synthetic  $\text{Ti}_3\text{O}_5$  (Onoda 1998), TiO (Loehman et al. 1969), and  $\text{TiO}_2$  (anatase, rutile, and brookite) reported in Ballirano and Caminiti (2001), Howard et al. (1992), and Meagher and Lager (1979).

The HKL software automatically suggests indexing solutions ranked by the lowest “mean angular deviation” (MAD) as an index of “goodness of fit.” MAD numbers <1 are considered desirable for accurate solutions, and each solution selected in this study was the highest ranked solution and exhibited a MAD number below 0.3. The patterns can be indexed only by the trigonal  $R\bar{3}c$   $\text{Ti}_2\text{O}_3$  structure to give a best fit based on unit-cell data (ICSD No. 77696, PDF 43-1033) from Vincent et al. (1980) (Fig. 4), showing  $a = 5.158 \text{ \AA}$ ,  $c = 13.611 \text{ \AA}$ ,  $V = 313.61 \text{ \AA}^3$ , and  $Z = 6$ , with the mean angular deviations as low as 0.27. No errors are stated because the cell parameters are taken directly from the data of the matching  $\text{Ti}_2\text{O}_3$  phase in Vincent et al. (1980).

X-ray powder-diffraction data were not obtained but can be estimated from data taken from PDF 43-1033, that were calculated from the cell parameters from Vincent et al. (1980) with MICRO-POWD v.2.2. The strongest calculated X-ray powder diffraction lines from the synthetic  $\text{Ti}_2\text{O}_3$  data are [ $d$  spacing in  $\text{Å}$  ( $hkl$ ): 3.734 (84) (012), 2.707 (88) (104), 2.579 (90) (110),

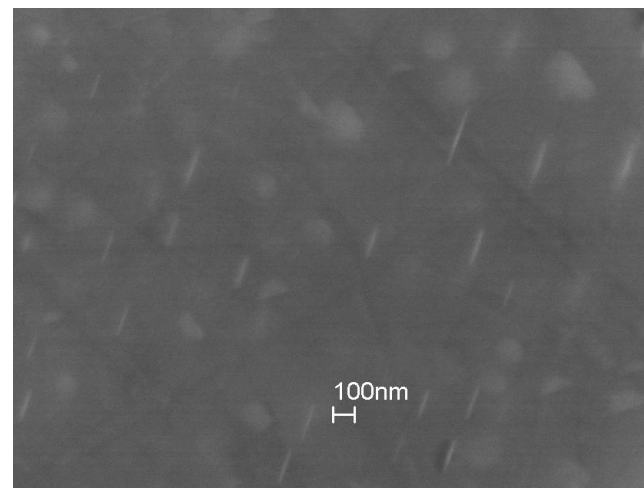


**FIGURE 3.** Nano-inclusions in this Allende tistarite grain.

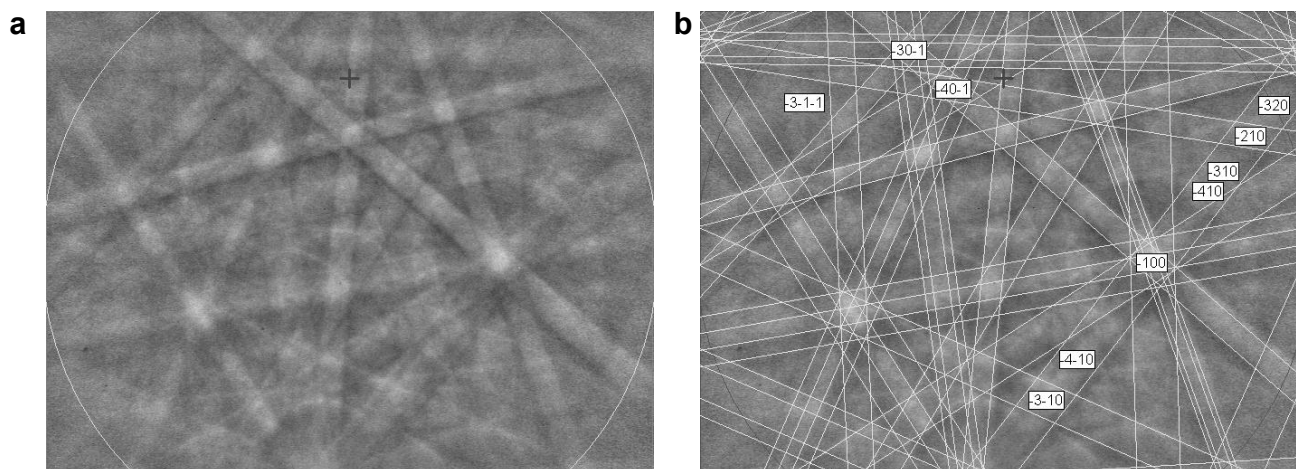


FIGURE 4. (a) Electron back-scattered diffraction pattern of the labeled Ti<sub>2</sub>O<sub>3</sub> crystal (marked with a cross) in Figure 2; (b) the pattern perfectly indexed with the rhombohedral  $R\bar{3}c$  Ti<sub>2</sub>O<sub>3</sub> structure.

2.242 (38) (113), 1.867 (33) (024), 1.703 (100) (116), 1.512 (28) (214), 1.489 (46) (300), 1.121 (20) (226), and 0.896 (25) (416).

#### SPECTROSCOPIC PROPERTIES

Raman spectroscopic microanalysis was carried out using a Renishaw M1000 micro-Raman spectrometer system on the tistarite crystal. Approximately 5 mw of 514.5 nm laser illumination (at the sample) focused with a 100× objective lens provided satisfactory spectra. The spot size was about 2 μm. Peak positions were calibrated against a silicon standard. A dual-wedge polarization scrambler was used in the laser beam for all spectra to minimize the effects of polarization. Raman analysis gave no indication of either H<sub>2</sub>O or CO<sub>2</sub> in tistarite. Raman microanalyses show that the spectrum of Allende tistarite (using a 514.5 nm laser) is similar to that of synthetic Ti<sub>2</sub>O<sub>3</sub> obtained from Cerac, Inc., as shown in Figure 5.

#### DISCUSSION

Tistarite (Ti<sub>2</sub>O<sub>3</sub>) belongs to the corundum-hematite group ( $A_2^{3+}O_3$  with the  $R\bar{3}c$  structure), which includes corundum (Al<sub>2</sub>O<sub>3</sub>), hematite (Fe<sub>2</sub>O<sub>3</sub>), eskolaite (Cr<sub>2</sub>O<sub>3</sub>), and karelianite (V<sub>2</sub>O<sub>3</sub>). This first occurrence of Ti<sub>2</sub>O<sub>3</sub> in nature is a refractory phase occurring near khamrabaevite (TiC) and corundum in Allende, a primitive meteorite. Previously discovered TiC grains in primitive meteorites have been found to be of presolar origin based on isotopic studies (Bernatowicz et al. 1991; Croat et al. 2003). Carbon isotope NanoSIMS analysis of the TiC grain near the tistarite did not indicate a definite presolar origin. Likewise, NanoSIMS oxygen isotope measurements on nearby corundum grains show that the grains have compositions well above the terrestrial fractionation line but on the carbonaceous chondrite anhydrous minerals line, consistent with formation or alteration in an <sup>16</sup>O-depleted reservoir within the solar system (Ma et al. 2009). The limited isotope measurements suggest that the cluster is probably not presolar. Tistarite is more likely a new condensate mineral formed under highly reducing conditions at the earliest stage of the solar system, less likely a new presolar mineral formed prior to the formation of the solar system. Because there is only one

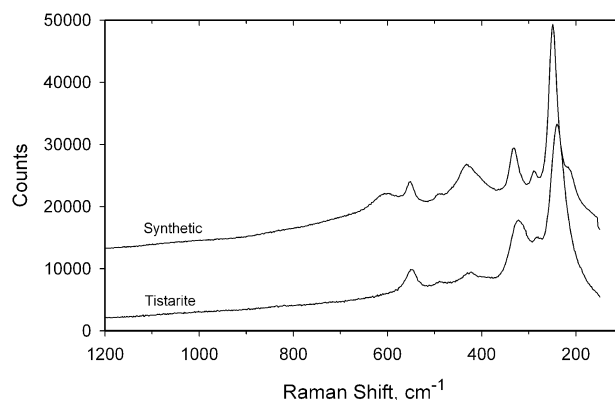


FIGURE 5. Raman spectra of Allende tistarite and synthetic Ti<sub>2</sub>O<sub>3</sub>.

micrometer-sized grain of tistarite found at this time, to protect the type-material grain deposited at the Smithsonian Institution, ion probe isotopic analyses have not been conducted.

Tistarite appears to be the first Ti-rich phase where Ti is totally in the 3+ oxidation state. Corundum grains in this cluster are Ti rich with 0.43–3.21 wt% Ti<sub>2</sub>O<sub>3</sub>. Minerals containing small amounts of Ti<sup>3+</sup> are well established. Ti-rich pyroxenes observed in Allende often have been interpreted to have Ti in both 4+ and 3+ oxidation states (Dowty and Clark 1973). Blue hibonite from a variety of meteorites such as Murchison, Murray, and Vigarano owes its color to mixed Ti<sup>3+</sup>-Ti<sup>4+</sup> oxidation states (Ihinger and Stolper 1986; Beckett et al. 1988). Larger amounts of Ti<sup>3+</sup> have been measured in an unnamed  $R^{2+}R_3^{4+}O_7-R_3^{3+}R_3^{4+}O_7$  solid-solution series where R<sup>3+</sup> is dominated by Ti (Haggerty 1978). Haggerty noted that the high Ti<sup>3+</sup> concentrations demonstrated that Ti<sup>3+</sup> was a significant constituent of the high-temperature condensings solar nebula.

Previously, there was speculation about color in minerals of terrestrial origin such as micas, pyroxenes and tourmalines arising from Ti<sup>3+</sup>. In most cases, later work has shown that the colors arise from Fe<sup>2+</sup>-Ti<sup>4+</sup> inter-valence charge transfer. Terrestrial Ti<sup>3+</sup>, however, has been found as a trace component in TiO<sub>2</sub> polymorphs where a small amount of Ti<sup>3+</sup> will cause an intense blue color in phases such as anatase and rutile (Chesnokov 1960).

Titanium in the 3+ oxidation state has again been demonstrated to be an important component in the Allende meteorite. Tistarite is the mineral with highest concentration of Ti<sup>3+</sup> found in nature.

#### ACKNOWLEDGMENTS

The Caltech GPS Analytical Facility is supported, in part, by grant NSF EAR-0318518 and the MRSEC Program of the NSF under DMR-0080065. Funding from NSF grant EAR-0337816 is also acknowledged. We thank the Smithsonian Institution for Allende sections.

#### REFERENCES CITED

- Armstrong, J.T. (1995) CITZAF: A package of correction programs for the quantitative electron microbeam X-ray analysis of thick polished materials, thin films, and particles. *Microbeam Analysis*, 4, 177–200.
- Ballirano, P. and Caminiti, R. (2001) Rietveld refinements on laboratory energy dispersive X-ray diffraction (EDXD) data. *Journal of Applied Crystallography*, 34, 757–762.
- Beckett, J.R., Live, D., Tsay, F.D., Grossman, L., and Stolper, E. (1988) Ti<sup>3+</sup> in meteoritic and synthetic hibonite. *Geochimica et Cosmochimica Acta*, 52, 1479–1495.
- Bernatowicz, T.J., Amari, S., Zinner, E.K., and Lewis, R.S. (1991) Interstellar grains within interstellar grains. *Astrophysical Journal*, 373, L73–L76.
- Chesnokov, B.V. (1960) Spectral absorption curves of certain minerals colored by titanium. *Academy of Sciences of the USSR* 129, 1162–1163. Translation of *Doklady Akademii Nauk, SSSR* 129, 647–649.
- Croat, T.K., Bernatowicz, T., Amari, S., Messenger, S., and Stadermann, F.J. (2003) Structural, chemical, and isotopic microanalytical investigations of graphite from supernovae. *Geochimica et Cosmochimica Acta*, 67, 4705–4725.
- Dowty, E. and Clark, J.R. (1973) Crystal structure refinement and optical properties of a Ti<sup>3+</sup> fassaite from the Allende meteorite. *American Mineralogist*, 58, 230–242.
- Haggerty, S.E. (1978) The Allende meteorite: Solid solution characteristics and the significance of a new titanate mineral series in association with armalcolite. *Proceedings of the 9<sup>th</sup> Lunar and Planetary Science Conference*, p. 1331–1344. Lunar and Planetary Institute, Houston.
- Howard, C.J., Sabine, T.M., and Dickson, F. (1992) Structural and thermal parameters for rutile and anatase. *Acta Crystallographica*, 47, 462–468.
- Ihinger, P.D. and Stolper, E.M. (1986) The color of meteoritic hibonite: An indicator of oxygen fugacity. *Earth and Planetary Science Letters*, 78, 67–79.
- Loehman, R.E., Rao, C.N.R., and Honig, J.M. (1969) Crystallography and defect chemistry of solid solutions of vanadium and titanium oxides. *Journal of Physical Chemistry*, 73, 1781–1784.
- Ma, C., Beckett, J.R., Rossman, G.R., Connolly Jr., H.C., Guan, Y., Eiler, J.M., and Hofmann, A.E. (2009) In situ discovery of a cluster of refractory grains in an Allende ferromagnesian chondrule. 40<sup>th</sup> Lunar and Planetary Science Conference, Lunar and Planetary Institute, Houston, Abstract 2138.
- Meagher, E.P. and Lager, G.A. (1979) Polyhedral thermal expansion in the TiO<sub>2</sub> polymorphs: Refinement of the crystal structures of rutile and brookite at high temperature. *Canadian Mineralogist*, 17, 77–85.
- Newnham, R.E. and de Haan, Y.M. (1962) Refinement of the α-Al<sub>2</sub>O<sub>3</sub>, Ti<sub>2</sub>O<sub>3</sub>, V<sub>2</sub>O<sub>3</sub>, and Cr<sub>2</sub>O<sub>3</sub> structures. *Zeitschrift für Kristallographie*, 117, 235–237.
- Onoda, M. (1998) Phase transitions of Ti<sub>2</sub>O<sub>3</sub>. *Journal of Solid State Chemistry*, 136, 67–73.
- Rice, C.E. and Robinson, W.R. (1977) High-temperature crystal chemistry of Ti<sub>2</sub>O<sub>3</sub>: Structural changes accompanying the semiconductor-metal transition. *Acta Crystallographica*, B33, 1342–1348.
- Vincent, M.G., Yvon, K., and Gruttner, A. (1980) Electron-density studies of metal-metal bonds. I. The deformation density of Ti<sub>2</sub>O<sub>3</sub> at 295 K. *Acta Crystallographica*, A36, 803–808.

MANUSCRIPT RECEIVED JANUARY 23, 2009

MANUSCRIPT ACCEPTED MARCH 11, 2009

MANUSCRIPT HANDLED BY BRYAN CHAKOUMAKOS